Appl. Phys. B 87, 445–449 (2007)
DOI: 10.1007/s00340-007-2611-0

Applied Physics B
Lasers and Optics

A. STOITA
S. GUY✉
B. JACQUIER

Measurement of the fraction of reabsorbed light in an Er^{3+}-doped glass

Laboratoire de Physico-Chimie des Matériaux Luminescents, Université Lyon,
UMR n5620 du CNRS, Domaine Scientifique de la Doua 10, rue André-Marie Ampère,
69622 Villeurbanne Cedex, France

Received: 18 October 2006/Revised version: 1 February 2007
Published online: 4 April 2007 •

ABSTRACT We report on an original continuous holographic grating technique to quantify the excitation transport within the excited states of erbium ions. We measure a very long range effect well beyond the μm distance which is attributed to radiation trapping. We demonstrate that 30% of the emitted light is reabsorbed inside the sample due to total internal reflections (TIR). The effect of reabsorption is totally removed when TIR are reduced by refractive index matching of the surroundings of the sample.

PACS 78.20.-e

1 Introduction

Radiation trapping is well known for lengthening the lifetime in rare earth-doped materials. This effect occurs for resonant transitions with a strong overlap between absorption and emission spectra. It is the result of the radiation transport (transport of the excitation via emission and absorption of photons) and total internal reflection (TIR) at the interfaces which traps the emitted light along infinite pathways [1–3]. The radiation trapping impact on the lifetime measurements has been specifically studied in two materials: Yb^{3+}:YAG [1, 2, 4] for which reported measured lifetimes vary from 950 μs to 1350 μs [2] and Er^{3+}:$LiNbO_3$ [3, 5] for which lifetime measurements spread from 2 ms up to 4.7 ms. It has been shown that these large uncertainties on the measured lifetimes are directly related to radiation trapping effect. Understanding and quantifying this effect will give useful information to accurately describe radiation properties of any luminescent material. We recently proposed a model describing lifetime lengthening in solid state materials [6] based on the fact that the radiation transport is mainly governed by TIR, which evens the energy re-deposition. It gives an analytical expression of the measured lifetime which strongly depends on the fraction of light reabsorbed inside the sample body, the ratio between the excitation/collection volume and the sample dimension. Thus, knowing both the fraction of reabsorbed light and the optical setup, it is possible to estimate the reliability of the lifetime measurements. The main unknown parameter is the fraction of reabsorbed light. Theoretically, for high symmetrical bodies, the part of trapped light from an emission inside the sample can be determined from geometrical consideration [7]. In experimental conditions, the overlap between absorption and emission, as well as sample imperfections, must be also taken into consideration.

This work presents the experimental quantification of the fraction of light reabsorbed in parallelepipedic materials. The sample is a 5 at. % erbium-doped fluoride ZBLA (ZrF_4-BaF_2-LaF_3-AlF_3) glass. It is an ideal candidate for investigating radiation trapping effects because of the long lifetime combined with the strong overlap between absorption and emission spectra of the two first excited states. In this paper we focus on the second excited state $^4I_{11/2}$ because:

1. it gets the energy transfer processes required for the experiment described below
2. it can be easily excited following a sine pattern with a single mode Ti:sapphire laser tuned at 800 nm.

We set up a continuous holographic grating technique similar to the four wave mixing experiment firstly proposed by Noginov et al. [8]. The key of the experiment is to measure the contrast of the erbium ion population excited by the laser grating through up-converted fluorescence. In our case, the sample is shined by a $\sim$ 800 nm light grating from a continuous wave single mode Ti:sapphire laser. This laser excitation provides a spatially distributed ion population in the $^4I_{11/2}$ metastable state, which is mainly radiative due to the low phonon energy of fluoride glasses matrix. By recording the up-conversion pumped green fluorescence from the $^4S_{3/2}$ level, we get the contrast of the sine pattern of the infrared metastable level $^4I_{11/2}$. Since the transport processes tend to erase the sine pattern, we obtain a direct quantification of the excitation transport between the erbium ions.

Two kinds of transports can occur in erbium-doped materials: the radiation transport (emission and absorption of photons further away in the sample) and the electric dipole–dipole energy transfer. Dipole energy transfer is a local diffusion process with a typical mean free path of around ten nanometers in rare-earth-doped materials which corresponds to a diffusion constant of $D = 10^{-10}$ cm^2/s for a 10 ms lifetime [8, 9]. On the other hand, the radiation transport is non-local and can spread over long distances as the emission may occur in

✉ Fax: +33 472 431130, E-mail: guy@pcml.univ-lyon1.fr

a wing of an absorption band [10]. Discrimination between diffusion and radiation transport can be done easily because these two transport processes occur at very different length scales.

In the first section, we will precise the order of magnitude of the propagation lengths by calculating the average transmission function of the resonant $^4I_{11/2} \leftrightarrow {}^4I_{15/2}$ transition. Then, because the radiation transport occurs at a long distance compared to the grating period, we may derive the expression of the contrast coefficient of the $^4I_{11/2}$ population grating in the presence of diffusion and radiation transport. The last section is devoted to the direct measurement of the fraction of reabsorbed light emitted from the $^4I_{11/2}$ level via the continuous up-conversion grating technique. At first, we identify the up-conversion mechanism responsible of the $^4S_{3/2}$ excitation and, finally, we show that the up-converted grating technique allows one to unambiguously measure a fraction of 30% of light reabsorbed in the sample.

2 Length scale of the radiation transport

For monochromatic radiation, the depth of propagation in an absorbing material depends on the absorption cross section following the Beer–Lambert law. In the case of a more complex emission profile, it is necessary to weight the Beer–Lambert law over the whole emission probability in order to get the average transmission function [10]

$$T(\varrho) = \int P_\mathrm{e}(\lambda)\mathrm{e}^{-N\sigma_\mathrm{a}(\lambda)\varrho}\mathrm{d}\lambda\,, \tag{1}$$

where ϱ is the propagation distance, σ_a is the absorption cross section and N the concentration. $P_\mathrm{e}(\lambda)$ is the normalized emission spectrum and is the probability that a photon is emitted at wavelength λ.

Figure 1 displays the absorption and emission spectra recorded on a Er^{3+}-doped ZBLA sample. The emission spectrum is normalized according to the following:

$$P_\mathrm{e}(\lambda) = b_\mathrm{r} I_\mathrm{e}(\lambda) / \int I_\mathrm{e}(\lambda)\mathrm{d}\lambda\,, \tag{2}$$

where b_r is the branching ratio of the $^4I_{11/2} \rightarrow {}^4I_{15/2}$ transition. This value is calculated to be 0.88 via standard a Judd-Ofelt procedure [11].

From these spectra the average transmission was calculated from (1) and is drawn in Fig. 2 for a 5 at. % doping level. The radiation transport over $^4I_{11/2} \rightarrow {}^4I_{15/2}$ resonant transition presents the general behaviour of radiation resonant transport: non-exponentiality and long range transport with 50% of the emitted photons still propagating after one centimeter path in the sample.

3 Erasing of a grating submitted to diffusion and radiation trapping

In this section we will quantify the washing out of an ion population continuously excited by a sine pattern. We consider the population as a two levels system and we take into account two different excitation transport processes: the local diffusion due to dipole–dipole interactions and the radiation transport for which the excitation moves from one point

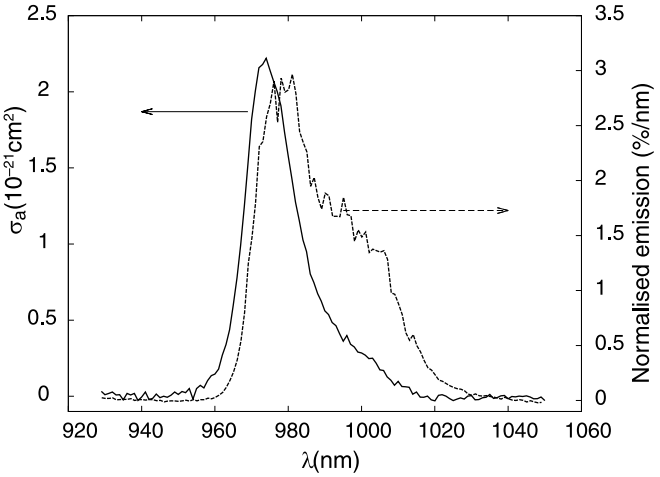

FIGURE 1 Absorption and emission spectra of the $^4I_{15/2} \leftrightarrow {}^4I_{11/2}$ transition in Er^{3+}:ZBLA. The emission spectrum is normalized so that the intensity value at λ is the probability per nanometer that a photon is emitted at λ

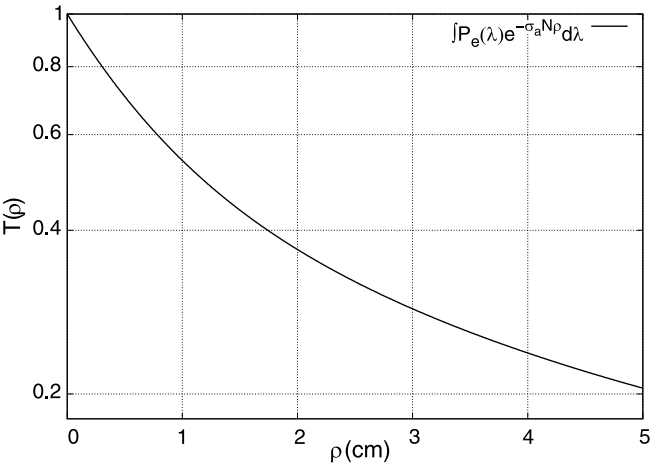

FIGURE 2 Average transmission $T(\varrho)$ (1) of the light emitted by the $^4I_{11/2}$ level as a function of the propagation distance inside a 5 at. % Er^{3+}-doped ZBLA glass

to another via emission and absorption of a resonant photon. The local diffusion phenomenon is described by the diffusion equation and, in the case of the rare-earth-doped materials, the mean free path is in the order of tens nanometers. The radiation transport is described by the so called Biberman–Holstein [10, 12] equation. In that case the transport is non-local because light emitted in the wing of the absorption band can propagate a long distance before being absorbed [10, 13]. In the steady state regime, the excited state population distribution is governed by the following equation:

$$0 = -\frac{n(\boldsymbol{r})}{\tau} + 2I_0\left[1+\sin\left(\frac{2\pi x}{\Lambda}\right)\right] + D\bigtriangledown^2 n(\boldsymbol{r}) + W_\mathrm{r}\int n(\boldsymbol{r}')G\left(|\boldsymbol{r}'-\boldsymbol{r}|\right)\mathrm{d}^3r'\,, \tag{3}$$

where the first term of the right-hand side represents the natural lifetime, the second one is the sine pattern of the laser excitation (Λ being the grating period), the third one takes into

account the local diffusion process. The radiation transport is described by the last integral term. The kernel function G, is the probability that a photon emitted at $\boldsymbol{r}'$ is absorbed at $\boldsymbol{r}$ and depends on the average transmission (1) following:

$$G(\varrho) = -\frac{1}{4\pi\varrho^2}\frac{\partial T}{\partial \varrho}\,. \tag{4}$$

To solve (3), we take advantage of the length scale of both the kernel function $G(r)$ and the sine function. The first one has typical length of the order of one centimeter (as it can be seen on Fig. 2), while the oscillating function is of the order of one micrometer. We are looking for a solution that takes the following form:

$$n(\boldsymbol{r}) = n(x) = n_0\left[1 + v\sin\left(\frac{2\pi x}{\Lambda}\right)\right]. \tag{5}$$

The important term is the contrast v, which measures how strongly the excited population leaves the excited region to go in the non-excited one's. We substitute expression (5) in (3) and separate the constant part from the sine part. Providing the fact that G varies slowly compared to the sine function, integration over the sine vanishes and then we have the following:

$$n_0 = 2\tau I_0 + \tau W_\mathrm{r} n_0 \int_{V_\mathrm{s}} G\mathrm{d}^3 r \tag{6a}$$

$$n_0 v = 2\tau I_0 - n_0\, v\tau D\left(\frac{4\pi^2}{\Lambda^2}\right), \tag{6b}$$

where V_s is the volume of the sample. The resolution is straightforward, giving a contrast reduction:

$$v = \frac{\Lambda^2}{\Lambda^2 + 4\pi^2\tau D}(1 - \eta f), \tag{7}$$

where $\eta = \tau W_\mathrm{r}$ is the quantum efficiency of the system, and f is the fraction of reabsorbed light inside the sample given by the formula

$$f = \int_{V_\mathrm{s}} G\mathrm{d}^3 r\,. \tag{8}$$

The expression of v shows that the reduction of the contrast is the product of two terms, the first one corresponds to the diffusion process [8] and the second one describes the fact that a fraction ηf of the sinusoidal pattern is reabsorbed uniformly in the sample. The discrimination between these two effects can be easily done because the first one depends strongly on the period of the grating while the second does not.

4 Light induced grating experiment

The determination of the reabsorbing factor can be performed directly by measuring the contrast of an ion population continuously excited via a grating pattern. The principle of this experiment was first described by Noginov et al. [8]. In our case, a continuous laser beam at ~ 800 nm from a highly coherent Ti:sapphire laser ($\Delta\nu = 40$ MHz) is split in two mutually coherent beams of equal intensity and waist (5 mm)

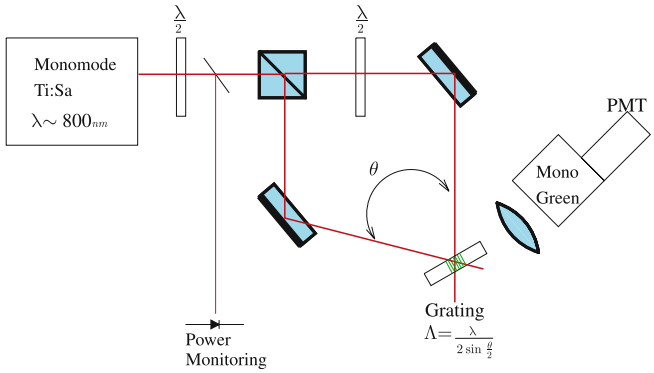

FIGURE 3 Experimental setup: The beam from the Ti:sapphire laser is split in two with a polarizing beam splitter before converging at some angle in the sample. The first $\frac{\lambda}{2}$ plate allows one to control the relative intensity of the two beams, the second one manages the coherence between the two incident beams

crossing at some angle (θ) on to the $4\times4\times1$ mm^3 piece of a 5 at. %Er^{3+}:ZBLA glass (Fig. 3). The polarization of the two beams is controlled with half wave plates and polarizers. 5% of the pump beam is split through a glass plate to monitor the intensity during the whole experiment. When the two beams are coherent (parallel polarisation), thanks to the fast phonon relaxation from the $^4I_{9/2}$ level, the pumping photons populate the $^4I_{11/2}$ energy level following a sine pattern. The distribution of the excited erbium ions deviates from the sine pattern following (5) because of the migration processes (diffusion or/and radiation transport).

As stated in [8], direct infrared fluorescence recording does not allow one to get information on the visibility factor, only up-converted fluorescence allows one to get the visibility information. Indeed, by collecting fluorescence one performs a spatial integration over the sample (mathematically speaking it corresponds to a spatial averaging over the excited population distribution). It is straightforward to see that the averaging of the excited population distribution (5) depends only on the averaged value and not on the oscillation amplitude (i.e., $\int_V (1 + v\sin)\mathrm{d}^3x = V$ providing that the integration volume includes many grating periods). For up-converted fluorescence, the doubly excited population depends quadratically on the directly excited population. This non-linearity also leads to non-linearities in spatial oscillations proportional to v^2 (A.6) which do not disappear by integration ($\int_V v^2\sin^2\mathrm{d}^3x = V\frac{v^2}{2}$).

We use the green up-converted fluorescence arising from the radiative relaxation of the $^4S_{3/2}$ energy level to determine the contrast coefficient. This light is collected through a monochromator and sent to a photomultiplier tube. For each angle, we measure successively the four green fluorescences: F_1 with only the first beam, F_2 with only the second beam; F_{coh} with the two beams mutually coherent (having parallel polarization) and F_{incoh} with the two beams incoherent (having perpendicular polarization). Assuming that the $^4S_{3/2}$ ion population varies quadratically with respect to the $^4I_{11/2}$ population, the up-converted fluorescence depends on the contrast coefficient v and the overlap between the two beams (see appendix A). The contrast coefficient v can be calculated from the measurements of F_1, F_2, F_{coh}, F_{incoh} from (A.9) of the appendix A.

4.1 *Identification of the up-conversion mechanisms*

In order to identify the up-conversion mechanisms responsible of the green emission, we have recorded the decay (Fig. 4) and the rise time (Fig. 5) of the different emissions under quasi continuous pumping excitation at 800 nm. The green light decay exhibits some non-linearity just after the laser is switched off, then it evolves exponentially with a lifetime of ∼3.4 ms. We have also recorded the natural decay of the $^4S_{3/2}$ with a pulsed excitation (10 ns width) provided by a pulsed OPO laser and found a lifetime of 40 μs. The decay recorded under a quasi continuous 800 nm excitation is then much longer than the natural decay . It is close to half of the $^4I_{11/2}$ lifetime which is the signature of the up-conversion energy transfer process. Moreover, we checked that the population of the $^4S_{3/2}$ state depends quadratically on the population of the $^4I_{11/2}$ multiplet by comparing the building up of these populations during the pumping regime as it can be seen in Fig. 5.

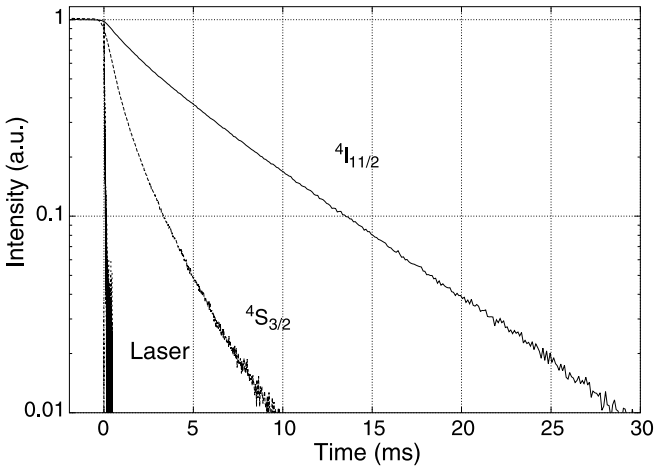

FIGURE 4 Decays of the fluorescences of the $^4I_{11/2}$ and $^4S_{3/2}$ energy levels after continuous excitation at 801 nm in the $^4I_{9/2}$ energy level

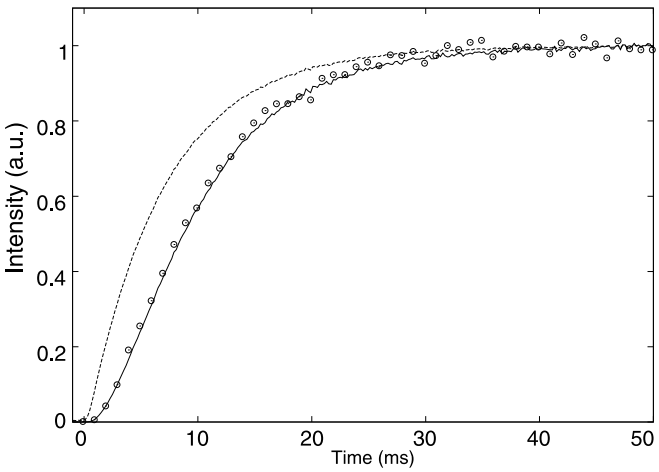

FIGURE 5 Rises of the fluorescence of the $^4I_{11/2}$ (*dashed curve*) and $^4S_{3/2}$ (*circles*) energy levels during quasi continuous excitation at 801 nm in the $^4I_{9/2}$ energy level. The continuous curve "underneath" the $^4S_{3/2}$ emission is the square of the intensity of the $^4I_{11/2}$ emission

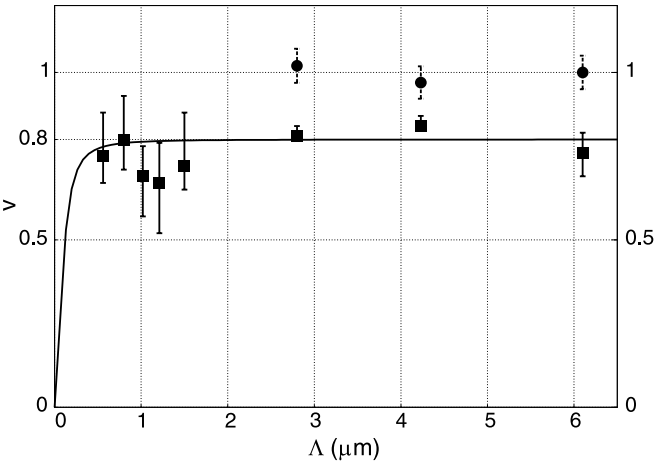

FIGURE 6 Variation of the contrast as a function of the grating period for the sample "in air" (*square*), and for the sample optically glued on an absorptive filter (*circle*). The error-bars correspond to 3 different experiments. The continuous curve is the plot of the theoretical expression of v (7) with $\tau = 7$ ms, $\eta f = 0.2$ and $D = 10^{-9}$ cm^2/s

4.2 *Results*

The dependence of v versus the angle between the two writing beams, θ, was deduced from the measurement of the four green intensity F_1, F_2, F_{coh} and F_{incoh} following (A.9) at each angle. The results of the measurements are presented in Fig. 6 (squares). The error bars are related to the fluctuations over three different experiments.

There is no dependence of the contrast with the grating period. Whatever the writing angle is, the contrast is reduced to the value $v = 0.8 \pm 0.05$. Thus, the erasing of the grating is due to a long range transport process. Here, long range means longer than the maximum grating period of ∼ 6 μm.

The effect of TIR was investigated by optically gluing the back face of the sample on a Schott NG3 ($l = 2$ mm, transmission = 4% at $\lambda = 1$ μm) absorbing filter with an index-matching liquid. In that case, most of the photons striking the bottom face of the sample penetrate the NG3 filter where they are absorbed and so can not circulate further away back in the sample. With this configuration, the contrast of the grating (circles in Fig. 6) is not affected showing that there is no redistribution of the energy inside the sample when the TIR are eliminated.

5 Discussion

The continuous grating experiment demonstrates that the Er^{3+} excitation is submitted to a long range transport process dominated by TIR. This is clearly the signature of radiation trapping. Our model allows one to extract the fraction of reabsorbed light from the experimental results. The continuous curve on Fig. 6 is the drawing of (7) with $\tau = 7$ ms, $\eta f = 0.2$ and $D = D_{lim} = 10^{-9}$ cm^2/s. Equation (7) depends on the two physical parameters ηf and D. Nevertheless, the sensitivity of the grating experiment to the diffusion parameter is limited by the minimum grating period. Indeed, (7) presents significant variation versus Λ only if the diffusion length ($l_d = 2\pi\sqrt{\tau D}$) is in the order of the magnitude of the grating period range. The continuous curve on Fig. 6

shows more precisely the limit of accuracy of our experimental setup: we are not able to detect value of D lower than D_{lim}. The actual value of D is obviously lower than D_{lim} as stated in Sect. 2.

Judd–Ofelt calculation and multiphonon transition probabilities determination lead to a quantum efficiency of the $^4I_{11/2}$ level in ZBLA of $\eta = 0.65$ [11]. Thus the fraction of reabsorbed light inside the sample is $\sim 30\%$. From Fig. 2, it corresponds to a propagating distance of 5 mm and therefore 5 TIR with respect to the smallest size of the sample. These values are compatible with Shurcliff and Jones's report [7] who calculated that 23% of the light is trapped in a parallelepiped rectangle of $n = 1.5$ because of infinite TIR paths. This value grows up to 74% for an infinite slab (closer to our geometry).

6 Conclusion

We show theoretically that the continuous holographic grating technique measures directly the nature of the excitation transport in the studied sample. Using this technique, we have determined that 30% of the light emitted by the $^4I_{11/2}$ level of Er^{3+} is reabsorbed inside a parallelepipedic sample of 5 at. %Er^{3+}:ZBLA, this reabsorption is governed by the TIR at the interfaces.

This is the first time, to our knowledge, that the measurement of the reabsorbed light inside a rare-earth-doped sample is done. The precise determination of reabsorbed light in luminescent materials and consequently the dynamics of the excited populations are of importance in the modeling of properties such as solid state lasers or amplifiers.

Appendix

A Calculation of the contrast

A.1 *beam intensity*

Two beams $\Phi_1(x, y, z)$ and $\Phi_2(x, y, z)$ are crossing inside the sample. If they are mutually coherent, the resulting intensity is a sine pattern of period Λ

$$\Phi_{\text{coh}} = \Phi_1 + \Phi_2 + 2\sqrt{\Phi_1\Phi_2}\sin\left(\frac{2\pi}{\Lambda}x\right), \tag{A.1}$$

where $\Lambda = \frac{\lambda}{2sin\frac{\theta}{2}}$.

If the two beams are incoherent, the resulting intensity is simply:

$$\Phi_{\text{incoh}} = \Phi_1 + \Phi_2 \tag{A.2}$$

A.2 *Direct fluorescence*

Assuming no saturation in the pumping process, the excited level population distribution is directly proportional to the intensity:

$$n(x) \sim \Phi_1 + \Phi_2 + 2v\sqrt{\Phi_1\Phi_2}\sin\left(\frac{2\pi}{\Lambda}x\right). \tag{A.3}$$

The measured fluorescence is the collection of photons coming from the whole sample. Mathematically speaking it is the integration of the previous equation. Because the integration over the sine vanishes, the resulting fluorescence intensity does not depend on the contrast and can be written simply as the following:

$$F_{\text{direct}} \sim \int \Phi_1 \mathrm{d}^3r + \int \Phi_2 \mathrm{d}^3r\,. \tag{A.4}$$

A.3 *Up-conversion fluorescence*

We assume that the population of the up-conversion pumped excited state depends quadratically on the population of the pumped excited state. For each beam alone, the up-converted fluorescence intensity is then given by the following:

$$F_i \sim \int \Phi_i^2 \mathrm{d}^3r, \tag{A.5}$$

where $i = 1, 2$ for the beam number 1 or 2. When the two beams are coherent the resulting up-converted fluorescence is:

$$F_{\text{coh}} \sim \int \left(\Phi_1 + \Phi_2 + 2v\sqrt{\Phi_1\Phi_2}\sin\left(\frac{2\pi}{\Lambda}x\right)\right)^2 \mathrm{d}^3r \tag{A.6}$$

To integrate this equation, we use the fact that the sine function varies very fast in comparison to the intensity functions so that the integrations over the sine function vanish and integrations over $\sin^2$ simplify in a $\times \frac{1}{2}$. Finally by using (A.5), we obtain

$$F_{\text{coh}} = F_1 + F_2 + 2\left(1 + v^2\right)\int \Phi_1\Phi_2 \mathrm{d}^3r\,. \tag{A.7}$$

In a similar way, for two incoherent beams the resulting up-converted fluorescence is

$$F_{\text{incoh}} = F_1 + F_2 + 2\int \Phi_1\Phi_2 \mathrm{d}^3r \tag{A.8}$$

Using (A.5), (A.7) and (A.8) it is easy to see that

$$1 + v^2 = \frac{F_{\text{coh}} - F_1 - F_2}{F_{\text{incoh}} - F_1 - F_2}\,. \tag{A.9}$$

REFERENCES

1 D.S. Sumida, T.Y. Fan, Opt. Lett. **19**, 1343 (1994)
2 M.P. Hehlen, OSA Trend. Opt. Photo. Adv. Solid State Lasers **1**, 530 (1996)
3 D.L. Zhang, E.Y.B. Pun, J. Appl. Phys. **94**, 1339 (2003)
4 M.P. Hehlen, J. Opt. Soc. Am. B **14**, 1312 (1997)
5 J.A. Munoz, B. Herreros, G. Lifante, F. Cusso, Phys. Stat. Solidi A **168**, 525 (1998)
6 S. Guy, Phys. Rev. B **73**, 144 101 (2006)
7 W.A. Shurcliff, R. Clark Jones, J. Opt. Soc. Am. **31**, 912 (1949)
8 M.A. Noginov, H.J. Caulfield, P. Venkateswarlu, M. Mahdi, Opt. Mater. **5**, 97 (1996)
9 S.N. Houde-Walter, P.M. Peters, J.F. Stebbins, Q. Zeng, J. Non-Cryst. Solids **286**, 118 (2001)
10 T. Holstein, Phys. Rev. **72**, 1212 (1947)
11 E. Lebrasseur, PhD thesis, Université Lyon 1, 1999
12 L.M. Biberman, Zh. Eksp. Teor. Fiz. **17**, 416 (1947)
13 C. van Trigt, Phys. Rev. **181**, 97 (1969)